Carbon nanotubes as nanoscale probes of the superconducting proximity effect in Pd-Nb junctions

Alexander Tselev, Yanfei Yang, Jian Zhang,* and Paola Barbara†
Department of Physics, Georgetown University, Washington, DC 20057, USA

Serhii E. Shafranjuk
Department of Physics and Astronomy, Northwestern University, Evanston, Illinois 60208, USA
(Received 13 May 2009; published 5 August 2009)

We study carbon nanotubes (CNTs) connected to Nb superconducting electrodes through a thin (less than 5 nm) Pd layer. We show that the carbon nanotubes form nanoscale point contacts detecting superconducting proximity effect via Andreev reflection, where an electron injected from the nanotube is reflected as a hole at the Pd/Nb interface and a Cooper pair forms in the Nb. Our data cannot be quantitatively explained by a single interface model, where only one interface between the CNT and a superconducting electrode is considered. Instead, we present a quantitative analysis that includes two separate interfaces—CNT/Pd and Nb/Pd—at each end of the CNT. The data can be used to determine the transparencies of the Pd/Nb and CNT/Pd interfaces.

DOI: 10.1103/PhysRevB.80.054504 PACS number(s): 74.78.Na, 73.63.Fg, 74.45.+c

I. INTRODUCTION

Due to their small diameter, carbon nanotubes (CNTs) offer unprecedented opportunities to study phase-coherent charge transport phenomena at the nanometer scale. In the case of carbon nanotubes connected to superconducting electrodes, examples include the interplay between superconductivity and Kondo effect,[1] Andreev reflection and multiple Andreev reflection at superconductor/CNT interfaces.[2,3] Nanoscale superconducting devices such as supercurrent transistors[4] and gated superconducting quantum interference devices[4] have also been demonstrated.

Earlier work on the subject was focused either on the Josephson effect[4–6] or on multiple Andreev reflections[2,3] with the requirement that the superconducting phase coherence had to be preserved through the whole device. Consequently, the CNT section connecting the electrodes had to be shorter than the phase-coherence length. By contrast, here we focus on the *local* phase-coherent properties of the carbon nanotube/electrode interface, and study how superconductivity is induced from a superconducting electrode (Nb) to the CNT through a thin (less than 5 nm) layer of a normal metal (Pd), using devices with relatively long CNT sections between electrodes, so that the superconducting phase coherence across the whole device is not established. Remarkably, our data indicate that in this regime, a carbon nanotube/electrode junction behaves as a nanoscale point contact detecting Andreev reflection at the superconductor/normal-metal interface.[7–10] (We note that since superconducting materials do not typically form highly transparent contacts with carbon nanotubes, a thin layer of Pd or Ti is usually applied between the superconductor and the nanotube to obtain highly transparent electrical contacts in CNT/superconducting junctions.[4–6,11,12])

In our experiment, where the thickness of the normal metal is smaller than the electron mean free path, and the diameter of the CNT point contact is smaller than the thickness of the normal layer, the charge-transport process can be pictured as follows. An electron injected from the CNT and undergoing Andreev reflection at the Pd/Nb interface is reflected as a hole. The hole follows the same path as the incoming electron (retroreflected), and consequently is focused back on the CNT, enhancing the current. By contrast, an electron injected from the CNT that undergoes conventional reflection at the Pd/Nb interface is deflected away from the CNT and does not contribute to the current (see Fig. 1).

The CNT thus detects the excess current due to the Andreev-reflected holes. This excess current causes the measured device differential conductance, G_s, to be higher than the normal conductance, G_n, (the conductance measured with Nb electrodes in the normal state). We have found that the ratio G_s/G_n does *not* depend on the gate voltage or G_n. Furthermore, we show that, since Andreev reflection depends only on properties of the CNT/Pd and Pd/Nb interfaces, the data can be used to determine the transparencies of these interfaces.

II. EXPERIMENTS

Our devices are carbon nanotube field effect transistors. They are fabricated on Si substrates, which are capped with ~350 nm-thick thermally grown dry Si oxide. The Si substrates are doped and are used as a back gate. Carbon nanotubes were grown by chemical vapor deposition. The source and drain electrodes were patterned by conventional photolithography and deposited by rf magnetron sputtering. A thin (2.5–5 nm) Pd layer was deposited directly onto nanotubes,

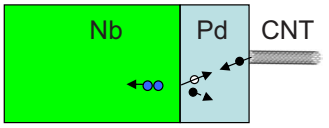

FIG. 1. (Color online) Carbon nanotube point contact: in the case of Andreev reflection, the retroreflected holes are focused back toward the nanotube whereas electrons undergoing normal reflection are deflected away from the nanotube.

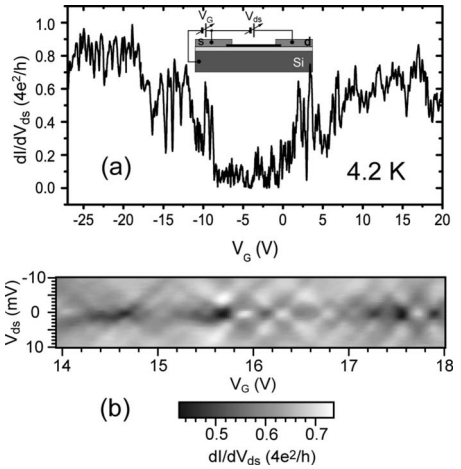

FIG. 2. (a) Zero-bias differential conductance vs gate voltage (V_G) in zero magnetic field at a temperature $T=4.2$ K. The inset shows the schematic of the CNT-field-effect transistor. (b) A gray-scale 2D map of differential conductance as a function of gate voltage (V_G) and bias (V_{ds}) at $T=4.2$ K in zero magnetic field. Brighter tone corresponds to higher conductance.

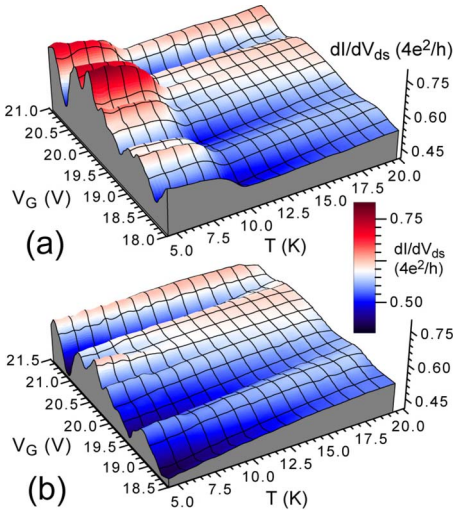

FIG. 3. (Color online) Surface plots of the zero-bias differential conductance as a function of gate voltage (V_G) and temperature (T): (a) in a magnetic field $B=0$ and (b) at $B=3$ T applied perpendicular to the substrate.

followed by deposition of a thick (about 200 nm) Nb layer.[13] The CNT length between the source and drain electrodes was between 1 and 5 μm. Differential conductance measurements were performed with an ac voltage level of 54 μVp-p. Here we present results for one particular sample. In this device the Pd layer was 3.5-nm thick, the Nb layer thickness was 200 nm and the carbon nanotube diameter and length were 1.5 nm and 1 μm, respectively. Similar results were obtained from four samples.

At low temperature, the zero-bias differential conductance as a function of the gate voltage V_G shows a dip and irregular oscillations [see Fig. 2(a)]. A two-dimensional (2D) map of dI/dV_{ds} versus V_G and drain-source bias voltage V_{ds} measured in a range of high conductance revealed a region with a clear oscillatory pattern characteristic of Fabry-Perot-type interference[14] as well as regions of conductance dips at zero bias surrounded by irregular patterns [see Fig. 2(b)]. These are signatures of energy-dependent resonant scattering at impurities or defects along the nanotube.[15,16]

The differential conductance when the Nb is superconducting ($T<9.0$ K in zero magnetic field) is greater than the differential conductance when the Nb is normal ($T>9.0$ K) for *all* values of the gate voltage. Figure 3(a) is a surface plot of conductance versus temperature and gate voltage, where the appearance of the excess conductance is manifested by a kink of the surface at the transition temperature of the leads. A magnetic field $B=3$ T, applied normal to the substrate, suppresses superconductivity in the whole temperature range, and the excess conductance is removed, which is evident from Fig. 3(b).

The magnetic field dependence of the differential conductance at fixed temperature ($T=4.2$ K) is shown in Fig. 4, in a range of gate voltage where the conductance is high. The conductance as a function of magnetic field is approximately constant after increasing the magnetic field above 1.5 T.

In Fig. 5(a) we plot differential conductance vs V_G curves obtained at $T=4.2$ K. The upper curve corresponds to the superconducting state of the electrodes (G_s) and the lower curve correspond to the electrodes in the normal state (G_n). If we multiply the curve G_n by a factor $\alpha=1.13$, we obtain the curve indicated by the open dots. Note that the open dots fall onto the upper curve, clearly indicating that G_s is proportional to G_n. Figure 5(b) shows similar curves corresponding to a positive range of gate voltage. Remarkably, the same factor $\alpha=1.13$ can be used to scale the curves, implying that the proportionality factor is independent of both V_G and G_n within a large conductance and gate voltage range. In the range of gate voltage with lowest conductance, at about $V_G=-5$ V, the uncertainty on the measured value of α was quite large, due to smaller signal-to-noise ratio, however we could estimate its value to be within the range $1.05<\alpha<1.3$. The factor α was smaller for other devices we measured, ranging from $\alpha=1.10$ for a device with similar thickness of the Pd layer to $\alpha=1.01$ for a device with a thicker (5 nm) Pd layer. A couple of devices with smaller thickness of Pd, about 2.5 nm, were only characterized at room temperature, because they showed very low conductance at all values of gate voltage.

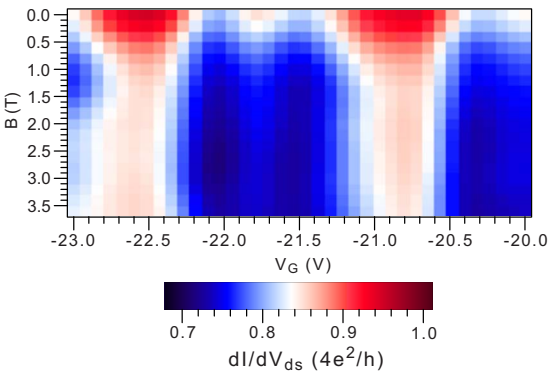

FIG. 4. (Color online) Zero-bias differential conductance as a function of gate voltage and magnetic field at $T=4.2$ K.

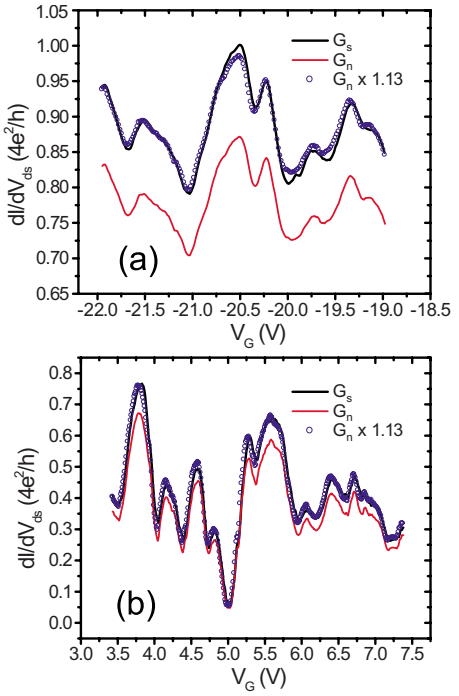

FIG. 5. (Color online) Zero-bias differential conductance vs gate voltage (V_G) at $T=4.2$ K. Upper solid curves in (a) and (b) were taken in zero magnetic field and lower solid curves were taken at $B=3$ T (Nb electrodes in the normal state). Open dots are the data of the lower curves multiplied a factor $\alpha=1.13$. Panels (a) and (b) correspond to greatly different ranges of the gate voltage V_G.

III. DATA ANALYSIS

A quantitative analysis of our data requires a detailed model of superconducting proximity effect in the contact region between the nanotube and the electrode. At first glance, it may seem reasonable to model the contact as a single interface between the carbon nanotube and a superconducting electrode, considering that the Pd layer is made superconducting by proximity effect. In this case, Andreev reflection occurs at the CNT/Pd interface. Electronic conduction in our nanotube is not ballistic because there are impurities or defects in the nanotube causing quantum interference effects and a strong dependence of the conductance G_n on gate voltage. The normal-state conductance can be expressed in terms of the Landauer-Büttiker formula, $G_n=4G_0T(E)$, where $G_0=e^2/h$ is the quantum conductance and $T(E)$ is the energy-dependent transmission. The formula accounts for the four one-dimensional (1D) channels conducting in parallel in a single-walled carbon nanotube due to spin degeneracy and the sublattice degeneracy of graphene. Benakker[17] has shown that, when considering Andreev reflection at the interface between a normal metal and a superconductor, quantum interference effects within the normal metal (the carbon nanotube in our case) lead to a strong dependence of the ratio G_s/G_n on the transmission $T(E)$. Therefore, according to this model, the ratio G_s/G_n should depend strongly on gate voltage. Our measurements, however, clearly show that the ratio G_s/G_n does not depend on gate voltage.

Here we propose a model that includes *two* interfaces,

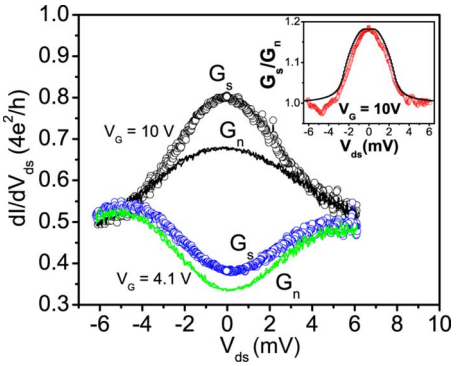

FIG. 6. (Color online) Pairs of curves of differential conductance vs bias (V_{ds}) for two different values of the gate voltage at $T=4.2$ K. Within each pair, the open dots correspond to zero magnetic field (superconducting electrodes) and the lines corresponds to $B=3$ T (normal electrodes). Inset: ratio of the superconducting state and normal-state differential conductances (G_s/G_n). The line is a fit to the experimental data (dots) using Eqs. (1) and (2) with $T_1=0.85$ and $T_2=0.8$.

CNT/Pd and Pd/Nb. In this model Andreev reflection occurs at the Pd/Nb interface, whereas the CNT/Pd interface is a major electron scatterer in the system, and it effectively "isolates" the CNT from the Pd/Nb interface. The carbon nanotube then acts as a point contact and detects excess current due to Andreev reflection at the Pd/Nb interface.[7,8] The superconducting state conductance G_s will be higher than the normal-state conductance, G_n, due to the retroreflected holes contributing to the current through the point contact. G_s will be proportional to G_n, with the ratio of the two values of conductance, at zero temperature, given by[8]

$$G_s/G_n = 1 + \varkappa A(eV_{pc}), \tag{1}$$

where V_{pc} is the voltage applied to the point contact and A is the energy-dependent Andreev reflection probability. The factor $\varkappa$ strongly depends on the transparencies of these interfaces.[18] In our case, V_{pc} should be considered as the voltage drop across one of CNT/electrode contacts. In the ideal situation of ballistic transport in the nanotube and identical contacts, the source-drain voltage across the device can be simply related to V_{pc} according to $V_{ds}=2V_{pc}$. Scattering in the nanotube will cause additional voltage drop along the nanotube and increase V_{ds} so that $V_{ds}>2V_{pc}$.

The bias dependence of the excess conductance is consistent with the two-interface point-contact picture. Regardless of the shape of the curves $G_{s,n}$ versus V_{ds} (peak or dip), the ratio G_s/G_n is a symmetric curve always peaked around $V_{ds}=0$ (see inset in Fig. 6). The smallest width of the peak in the G_s/G_n vs V_{ds} curves is about 3 mV and occurs at gate voltages where the transparency of the sample is highest, i.e., scattering within the nanotube is negligible and the voltage drop across the sample (V_{ds}) is approximately equal to the sum of the voltage drops across the two CNT/electrode contacts. The smallest width of the peak corresponds to roughly twice the superconducting gap of Nb, as is expected for two Pd/Nb interfaces in series.

The shape of the G_s/G_n versus bias curves with a peak at $V_{ds}=0$ indicates very transparent Pd/Nb interfaces with a high probability of Andreev reflection.[10] We note that, with highly transparent interfaces, the probability of Andreev reflection is high, and one would expect the current in the superconducting state to be close to the ideal limit with no interface barrier, i.e., twice as large as that in the normal state. However, in our device the current in the superconducting state increases only by about 13%. This low value of the excess current can be understood if we take into account that not all the retroreflected holes reach the nanotube. In our case, a finite potential barrier at the Pd/CNT interface is most likely the main factor preventing the retroreflected holes from getting back into the CNT.

In Fig. 6, we fit the measured excess conductance using a point-contact model for each end of the nanotube. We assume that the device is symmetric, namely, that the effective transparency of each nanotube/electrode contact, T_{end}, is the same at both ends (in the case of devices that are not symmetric, different transparencies for each end can be included in the model). Assuming that the nanotube/electrode contacts act as two identical incoherent scatterers, the total transparency due to the contacts is given by $T=T_{\mathrm{end}}/(2\text{-}T_{\mathrm{end}})$. The total resistance of the device can then be modeled as the sum of the quantized contact resistance and the intrinsic resistance of the barriers at the end, $G^{-1}=h/4e^2(1+2R_{\mathrm{end}}/T_{\mathrm{end}})$, where $R_{\mathrm{end}}=1\text{-}T_{\mathrm{end}}$.[19] We note that the assumption of a symmetric device is consistent with our experimental data since the high conductance indicates that the total transparency of the sample is close to the ideal case ($T=1$). Such high transparency cannot be achieved unless both ends are very transparent with asymmetry smaller than about 10%.

To calculate the effective nanotube/contact transparency T_{end}, we assume that the transport is fully coherent in vicinity of the Nb/Pd and Pd/CNT interfaces and also across the normal Pd layers (the phase coherence breaks inside the CNT section). We note that here we neglect unconventional interband processes, such as specular Andreev reflection,[20] which have been predicted to occur in graphene. We use the point-contact model described by Eq. (1), where at zero temperature the energy-dependent Andreev reflection coefficient is $A(\varepsilon)=(\xi-\varepsilon)/(\xi+\varepsilon)$, ε is the electron energy, and $\xi=\sqrt{\varepsilon^2-\Delta^2}$ is the electron kinetic energy. The factor $\varkappa$ is calculated using the Landauer-Büttiker formalism and the scattering matrix (S-matrix) technique[19] for electron and hole transport at the electrode/nanotube contact. The contact is modeled as an SI_1NI_2C junction (S is the superconducting electrode, N is the normal layer, C is the CNT section, $I_{1(2)}$ are the S/N and N/C interface barriers) and, for each 1D channel in the nanotube, Andreev reflection at the S/N interface is introduced using the BTK model.[10] The scattering matrix for the contact, S_{END} is composed of the partial 4×4 S matrices as $S_{\mathrm{END}}=S_S\otimes S_{I1}\otimes S_N\otimes S_{I2}\otimes S_C$, where S_S, $S_{I1(2)}$, S_N, and S_C are the S matrices of the superconductor, the barriers, the normal metal, and the carbon nanotube, respectively. The calculation yields $\varkappa=|\kappa|^2$, with

$$\kappa = 2T_2(\varepsilon+\xi)e^{-i(\phi+\phi_1+\phi_2)/2}/\mathcal{D}_\varepsilon, \tag{2}$$

where $\mathcal{D}_\varepsilon=4\xi+\xi\sqrt{1-T_2}Z_1^2(2-4T_2)-T_2^2Z_1^2\xi+8T_2^2(\xi+\varepsilon)-2T_2(5\xi+3\varepsilon)+2Z_1^2\xi$, T_2 is the N/CNT interface transparency, $Z_1=2\sqrt{(1-T_1)/T_1}$, T_1 is the normal-state S/N interface transparency, ϕ_1, ϕ_2, and ϕ are the electron wave-function phase shifts at the $I_{1(2)}$ barriers and in the N layer, respectively. The phase factors play a role when computing the conductance in magnetic field or the Josephson current while they cancel in Eq. (1). From the fit, we extract the interface transparencies $T_1=0.85$ and $T_2=0.8$. The theoretical solid curve in the inset of Fig. 6 is normalized to the normal-state voltage-dependent conductance $G_n(V_{ds})$. We also examined the contribution of inelastic scattering and the role of the junction inhomogeneity by introducing an imaginary part of the energy gap Γ. We find that, if $T_1\geq0.85$, which is the case in our experiment, the zero-bias peak does not depend much on Γ. Detailed calculations show that for devices with lower S/N interface transparency, $T_1<0.7$ and Γ set below 0.1 (in units of energy gap Δ), additional conductance sidepeaks would appear at $V_{ds}=\pm\Delta/e$.

IV. CONCLUSIONS

We study superconducting proximity effect in carbon nanotubes contacted by superconducting electrodes (Nb) through thin (less than 5 nm) Pd layers. In contrast to Refs. 4 and 5, where supercurrent through CNTs was observed, our nanotubes are longer than the phase-coherence length. Nevertheless, high interface transparency ensures that the excess current is not suppressed as it would be in the case of a low-transparency tunnel junction.[21] Phase-coherence persists along the electron-hole trajectory across the Pd layer and extends into the Nb electrodes and into the nanotube. The phase-coherent current is converted to a normal current deeply inside the nanotube, where there is no Cooper coupling and the phase coherence is eventually destroyed due to inelastic scattering. Under these conditions the carbon nanotube behaves as a local probe for superconducting proximity effect at the CNT/Pd/Nb interfaces and the point-contact behavior can be used to determine CNT/Pd and Pd/Nb interface transparencies.

ACKNOWLEDGMENTS

The authors gratefully thank I. Mazin, R. Gonnelli, and C. J. Lobb for fruitful discussions and the CNAM at the University of Maryland for the use of their facilities. This work was supported by the NSF (Grants No. DMR-0239721 and No. DMR-0521170).

*Present address: MicroMaterials, Inc. 13302 Telecom Drive, Tampa, Florida 33737.
†barbara@physics.georgetown.edu

[1] M. R. Buitelaar, T. Nussbaumer, and C. Schönenberger, Phys. Rev. Lett. **89**, 256801 (2002).
[2] M. R. Buitelaar, W. Belzig, T. Nussbaumer, B. Babić, C. Bruder, and C. Schönenberger, Phys. Rev. Lett. **91**, 057005 (2003).
[3] H. I. Jørgensen, K. Grove-Rasmussen, T. Novotný, K. Flensberg, and P. E. Lindelof, Phys. Rev. Lett. **96**, 207003 (2006).
[4] P. Jarillo-Herrero, J. A. van Dam, and L. P. Kouwenhoven, Nature (London) **439**, 953 (2006).
[5] J.-P. Cleuziou, W. Wernsdorfer, V. Bouchiat, T. Ondarçuhu, and M. Monthioux, Nat. Nanotechnol. **1**, 53 (2006).
[6] A. Y. Kasumov, R. Deblock, M. Kociak, B. Reulet, H. Bouchiat, I. I. Khodos, Y. B. Gorbatov, V. T. Volkov, C. Journet, and M. Burghard, Science **284**, 1508 (1999).
[7] P. A. M. Benistant, A. P. van Gelder, H. van Kempen, and P. Wyder, Phys. Rev. B **32**, 3351 (1985).
[8] D. R. Heslinga, S. E. Shafranjuk, H. van Kempen, and T. M. Klapwijk, Phys. Rev. B **49**, 10484 (1994).
[9] A. F. Andreev, Sov. Phys. JETP **19**, 1228 (1964).
[10] G. E. Blonder, M. Tinkham, and T. M. Klapwijk, Phys. Rev. B **25**, 4515 (1982).
[11] A. Javey, J. Guo, Q. Wang, M. Lundstrom, and H. Dai, Nature (London) **424**, 654 (2003).
[12] D. Mann, A. Javey, J. Kong, Q. Wang, and H. Dai, Nano Lett. **3**, 1541 (2003).
[13] A. Tselev, K. Hatton, M. S. Fuhrer, M. Paranjape, and P. Barbara, Nanotechnology **15**, 1475 (2004).
[14] W. Liang, M. Bockrath, D. Bozovic, J. H. Hafner, M. Tinkham, and H. Park, Nature (London) **411**, 665 (2001).
[15] M. Bockrath, W. Liang, D. Bozovic, J. H. Hafner, C. M. Lieber, M. Tinkham, and H. Park, Science **291**, 283 (2001).
[16] M. R. Buitelaar, A. Bachtold, T. Nussbaumer, M. Iqbal, and C. Schönenberger, Phys. Rev. Lett. **88**, 156801 (2002).
[17] C. W. J. Beenakker, Phys. Rev. B **46**, 12841 (1992).
[18] Since the ratio α does not depend on the gate voltage, we infer that the gate voltage does not alter the transparency of the Pd/CNT interface which is expected for a small bandgap nanotube without a Schottky barrier at the interface (Ref. 22).
[19] S. Datta, *Electronic transport in mesoscopic systems* (Cambridge University Press, Cambridge, New York, 1995).
[20] C. W. J. Beenakker, Rev. Mod. Phys. **80**, 1337 (2008).
[21] T. Kontos, M. Aprili, J. Lesueur, X. Grison, and L. Dumoulin, Phys. Rev. Lett. **93**, 137001 (2004).
[22] G. Fedorov, A. Tselev, D. Jimenez, S. Latil, N. G. Kalugin, P. Barbara, D. Smirnov, and S. Roche, Nano Lett. **7**, 960 (2007).